Extended X-ray Absorption Fine Structure Studies on the Iron-Containing Subunit of Ribonucleotide Reductase from *Escherichia coli*†

G. Bunker,*,‡ L. Petersson,§ B.-M. Sjöberg,∥ M. Sahlin,§ M. Chance,‡ B. Chance,‡ and A. Ehrenberg§

Institute for Structural and Functional Studies, Philadelphia, Pennsylvania 19104, Department of Biophysics, Arrhenius Laboratory, University of Stockholm, S-10691 Stockholm, Sweden, and Department of Molecular Biology, Swedish University of Agricultural Sciences, Uppsala Biomedical Center, S-75124 Uppsala, Sweden

Received October 27, 1986; Revised Manuscript Received March 20, 1987

ABSTRACT: Iron K-edge X-ray absorption spectra were obtained on the protein B2, the small subunit of ribonucleotide reductase from *Escherichia coli*. Protein B2 contains a binuclear iron center with many properties in common with the iron center of oxidized hemerythrins. The extended X-ray absorption fine structure (EXAFS) measurements on protein B2 were analyzed and compared with published data for oxyhemerythrin. In protein B2 there are, in the first coordination shell around each Fe atom, five or six oxygen or nitrogen atoms that are directly coordinated ligands. In oxyhemerythrin there are six ligands to each iron. As in oxyhemerythrin, one of the ligands in the first shell of protein B2 is at a short distance, about 1.78 Å, confirming the existence of a μ-oxo bridge. The other atoms of the first shell are at an average distance of 2.04 Å, which is about 0.1 Å shorter than in oxyhemerythrin. In protein B2 the Fe–Fe distance is in the range 3.26–3.48 Å, and the bridging angle falls between 130 and 150°. On the basis of these data, there is no direct evidence for any histidine ligands in protein B2, but the noise level leaves way for the possibility of a maximum of about three histidines for each Fe pair. The X-ray absorption spectrum of a hydroxyurea-treated sample was not significantly different from that of the native protein B2, which implies that no significant alteration in the structure of the iron site occurs upon destruction of the tyrosine radical.

Enzymatic reduction of ribonucleotides is an essential step in the biosynthesis of DNA. A controlled supply of the different deoxyribonucleotides is obtained through the catalytic action of ribonucleotide reductase (Thelander & Reichard, 1979). In nature, especially among microorganisms, there are several structurally and mechanistically different types of this enzyme. Iron-dependent reductases have been found or postulated for such diverse sources as animals, viruses, procaryotic organisms, and bacteriophages (Lammers & Follman, 1983). The reductase from *Escherichia coli* has been studied in considerable detail and can in several respects serve as a prototype for the others.

The enzyme in *E. coli* contains two subunits, B1 and B2, which both contribute to its active site. The B1 subunit has common binding sites for the four ribonucleotide diphosphate substrates and contains redox-active sulfhydryl groups. Allosteric effector sites on this subunit allow control of enzyme activity and substrate specificity. Protein B2 is made up of two identical polypeptide chains. It contributes a stable organic free radical (Ehrenberg & Reichard, 1972; Sjöberg & Gräslund, 1983) on tyrosine-122 (Larsson & Sjöberg, 1986) in one of the polypeptide chains. The tyrosyl radical, which is a necessary prerequisite for an active enzyme, is stabilized by a dimeric iron center. Information on this center has been obtained by means of different spectroscopic techniques (Atkin et al., 1973; Petersson et al., 1980; Sjöberg et al., 1982) and through magnetic susceptibility studies (Petersson et al., 1980). A remarkable resemblance is found to the iron center of oxidized forms of hemerythrin, an oxygen-transporting protein in several lower invertebrates. X-ray crystallographic studies on methemerythrin and metazidohemerythrin (Stenkamp et al., 1984) have verified a structure with a μ-oxo-bridged iron pair (Fe^{3+}–O^{2-}–Fe^{3+}). Two additional bridges are provided by the carboxylate groups on aspartate and glutamate residues in the protein. One of the iron atoms is further coordinated to three histidine nitrogens. The other iron has two histidine ligands and one position available for exogenous ligands like OH^-, N_3^-, etc. In oxyhemerythrin O_2^{2-} is bound to this position. X-ray absorption studies (Elam et al., 1982; Hendrickson et al., 1982) show a distance around 1.77–1.79 Å for the short Fe–O bond in oxy-, metazido- and methydroxohemerythrins.

Preliminary crystallographic data have been obtained for the small subunit of ribonucleotide reductase from *E. coli* (Joelson et al., 1984). Since no three-dimensional structure is available so far, little is, however, known about the ligand structure of its iron center. A comparison of amino acid sequences for the iron-containing subunit of reductases from four different species (Sjöberg et al., 1985), however, indicates potential iron ligands. In this study it was also suggested that the iron center is located at the interface between the two polypeptide chains of protein B2.

In the present paper,[1] we present X-ray absorption data on the B2 subunit of the reductase from *E. coli*. Our data are in agreement with a μ-oxo-bridged structure for its iron center as previously inferred from spectroscopic and magnetic studies (Atkin et al., 1973; Petersson et al., 1980; Sjöberg et al., 1982),

† Supported by grants from the Swedish Medical (B.-M.S.) and Natural Science (L.P. and A.E.) Research Councils and the Magn. Bergvall Foundation (B.-M.S.), in addition to NIH Grants GM-31992, HL-31909, HL-18708, GM-33165, and RR-01633 (G.B., M.C., and B.C.).

‡ Institute for Structural and Functional Studies.
§ University of Stockholm.
∥ Swedish University of Agricultural Sciences.

[1] A preliminary note on this work has previously been presented at the American Society of Biological Chemists (ASBC) meeting, Washington, DC (Bunker et al., 1986).

0006-2960/87/0426-4708$01.50/0

and the presence of a short Fe–O bond is verified.

Materials and Methods

Sample Preparation and Assay of Radiation Damage. Homogeneous protein B2 was obtained from *E. coli* cells carrying the recombinant plasmid pBS1, which overproduce the B2 subunit (Sjöberg et al., 1986). The preparation was 2.4 mM in protein B2, obtained in a buffer of 50 mM Tris-HCl, pH 7.6, and 20% glycerol. The radical content was 1.1 ± 0.1 mol/mol of protein and the specific activity was 6300 units/mg of protein (Sjöberg et al., 1986). In subsequent measurements, samples were prepared as described above but without addition of glycerol. The same batch of active preparation was divided into two parts. A 10 molar excess of hydroxyurea was added to one portion and the resultant mixture incubated at room temperature for 15 min to destroy the radical. The other portion received no hydroxyurea. The hydroxyurea was then removed from the sample by ultradialysis against buffer. Visible absorption data indicated a complete lack of the 410-nm band for the hydroxyurea-treated sample, indicating effective reduction of the tyrosine radical.

Prior to the EXAFS experiments ethylene glycol was added to the sample to avoid artifacts from diffraction by ice crystallites. The final concentration of ethylene glycol was 30%. Visible reflectance spectra, recorded on the frozen EXAFS sample, revealed no major changes as a result of the exposure to X-rays. At the end of the experiment, the radical absorption band at 410 nm was still clearly visible for the non-hydroxyurea-treated sample.

X-ray Absorption. The protein B2 X-ray absorption spectra were measured at the Stanford Synchrotron Radiation Laboratory (SSRL) Beam Line II-2 in July 1985 and June 1986. Silicon 111 crystals and a focusing mirror were used. The detector system consisted of an array of seven plastic scintillators/photomultiplier tube detectors with discriminators and amplifiers. Manganese oxide filters were used for background suppression. The electron beam energy and current were 3.0 GeV and <60 mA. A sample temperature of approximately 200 K during the data acquisition was obtained by flowing over the sample a stream of cold nitrogen gas from a liquid nitrogen temperature heat exchanger. The temperature of the flowing gas adjacent to the sample was measured with a thermocouple. Oxyhemerythrin and the model compounds used as standards and listed below were measured as described by Elam et al. (1982). In the following, we refer to the model compounds by short names. Their formulas are given: Fe glycine (Thundathil et al., 1977) is $[Fe_3O(glycinato)_6(H_2O)_3](ClO_4)_7$; Fe PDC (Ou et al., 1978) is $[Fe_2O(4\text{-chloro-2,6-pyridinedicarboxylate})_2(H_2O)_4]\cdot 4H_2O$; Fe TIM (Elam et al., 1982) is bis(acetonitrile)(2,3,9,10-tetramethyl-1,4,8,11-tetrazacyclotetradeca-1,3,8,10-tetraene)iron(II) hexafluorophosphate.

Data Analysis. EXAFS data were analyzed in the standard manner (Stern et al., 1975; Lee et al., 1981; Bunker & Sayers, 1986) using the University of Washington EXAFS program library with local enhancements. The spectra were summed, normalized to unit edge step, interpolated to k space, the background was approximated by a cubic spline and subtracted out, and the signals from different coordination shells were isolated by Fourier filtering. The resulting phases and amplitudes were then analyzed by nonlinear fitting methods, as well as the ratio method (Stern et al., 1975; Bunker, 1983). Beat analysis (Martens et al., 1977) was performed when appropriate.

Empirical back-scattering functions obtained from model compounds were used throughout the analysis, which is based on the standard EXAFS equation (Stern, 1974):

$$X(k) = \frac{\mu(E) - \mu_0(E)}{\mu_0(E)} = \sum_j \frac{N_j B_j(k)}{r_j^2} e^{-2k^2\sigma_j^2} e^{-2r_j/\lambda(k)} \sin [2kr_j + \delta_j(k)] \quad (1)$$

The quantities N_j, r_j, and σ_j^2 are respectively the coordination number, average distance, and mean square variation in distance to coordination shell j. The quantities $B_j(k)$ and $\delta_j(k)$ depend on the nature (atomic number) of the absorber and back-scatterer. They are determined from standards of known structure. $\lambda(k)$ is the photoelectron mean free path (the effect of which cancels out when standards and unknown are compared). It should be mentioned that if the product $k\sigma$ approaches 1 within the data range, eq 1 may break down. This is remedied by either including additional terms in eq 1 (Bunker, 1983) or repartitioning the atoms into coordination shells so as to reduce the σ^2. These practices are implicitly followed when necessary in this paper.

The spectra of protein B2 in this work and those of oxyhemerythrin and the standards (Elam et al., 1982) were measured under somewhat different conditions. To minimize systematic errors, small corrections to compensate for differences in energy resolution were estimated by convoluting the spectrum of the Fe glycine standard with Gaussians of 1.7, 4.2, and 6.1 eV full-width at half-maximum and analyzing the first, second, and third shell signals. For the third shell, the 4.2-eV broadening, which is a reasonable estimate of the resolution width for the protein B2 spectra, resulted in a 5% reduction in amplitude at $k = 2.8$ Å^{-1} and a 2% reduction at $k = 8.5$ Å^{-1}. The amplitude reduction was less than 2% for the first shell at $k = 2.8$ Å^{-1}. These corrections are substantially smaller than the error limits quoted below.

Since these initial protein B2 data were of limited signal-to-noise ratio for $k > 8.5$ Å^{-1}, it was important to minimize and estimate the effects of the noise. To help to estimate the parameter errors, two independent partial sums that comprised five and four scans, and also the total sum of nine scans, were analyzed in parallel. In nonlinear fitting, noise estimates were also independently obtained from the residual sum of squares function in the standard way (Lee et al., 1981). The quantity minimized was a weighted sum of the sums of squares of the phase and amplitude residuals. The quality of fits was confirmed by eye in all cases. Over 100 fits were performed with various initial starting values. Convergence to the same solution within round-off error always occurred after moderate change of the starting points. An approximate covariance matrix was calculated by inverting the Hessian (curvature) matrix and scaling by the noise level. The parameter correlation matrix and error limits that account for such correlations were then obtained from the covariance matrix. The error limits determined in this way were usually but not always consistent with the ones determined from the partial sums. It should be mentioned, however, that this method of estimating the covariance matrix is not strictly valid for filtered data, and therefore it was complemented by the partial sum method. When error limits determined by alternate methods differed significantly, the larger (more conservative) values were used. Additional errors incurred from the data reduction process and nonconsistency between standards were folded into the final error bars quoted.

Prior to summation of the scans, the spectra were inspected for artifacts (glitches) and energy shifts, which can arise from changes of the electron beam position between "fills". No energy shifts were observed, and only minimal deglitching

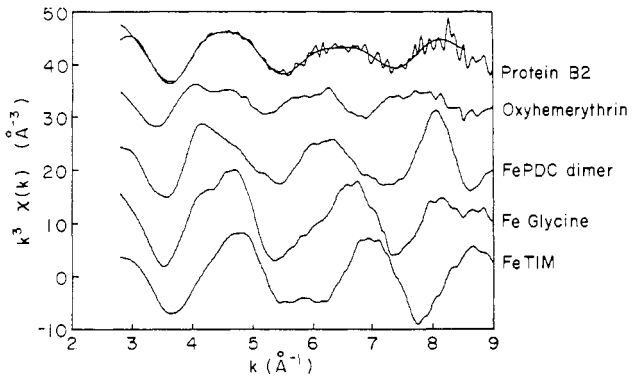

FIGURE 1: EXAFS data of ribonucleotide reductase subunit B2 (protein B2), oxyhemerythrin, and standards Fe TIM, Fe PDC, and Fe glycine after background subtraction and weighting by k^3. For protein B2 Fourier-smoothed data are overplotted. Oxyhemerythrin contains a μ-oxo bridge iron center (Fe^{3+}–O^{2-}–Fe^{3+}), and dioxygen is bound as O_2^{2-} to one iron. Fe glycine and Fe PDC contain Fe^{3+}, and Fe TIM contained Fe^{2+}.

(deletion of one or two individual points) was necessary. The portion of the spectrum in which the noise dominated the signal was not used. The usable data range extended from k = 2.8 to 8.5 Å^{-1}. This relatively short range required special attention to systematic errors from Fourier filtering distortions, and care was taken to ensure that these approximately cancelled out when protein B2 and the standards were compared. In particular, precisely the same k-space windows, and the same R-space window widths were used when comparing filtered data using nonlinear fitting and the ratio method.

After summation of the spectra, the edge steps were determined from the difference between preedge and postedge linear fits, extrapolated to the edge. Initially the energy threshold E_0 was set to 7109.0 eV for all spectra, which is in the preedge region (close to the 3d transition). The relative E_0 values were adjusted slightly (ca. 3 eV) in later analysis. The background was then subtracted over the range k = 2.8–8.5 Å^{-1}, by a three-region cubic spline with the function value and first two derivatives continuous at the junctures ("knots"). The residuals in this fit were weighted with k^3. Inspection of the derivative of the background fit showed that a negligible amount of the first shell signal was removed. The resulting EXAFS data (weighted with k^3) are shown in Figure 2.

RESULTS

EXAFS: Qualitative Analysis. Spectra of protein B2 were compared with those of the hydroxyurea-treated form. This comparison was accomplished by a least-squares fitting procedure to vary a multiplicative scale factor and a background curve (quadratic in energy relative to the edge) until best agreement was achieved between the spectra of native and hydroxyurea-treated protein B2. No differences were observed apart from noise. This null result indicates that there is no significant change in the structure of the iron center upon scavenging of the tyrosine radical.

The k^3-weighted EXAFS data for protein B2 shown in Figure 1 evidently contain substantial noise. Fortunately much of this noise is of sufficiently high frequency in k space that it is outside the pass band of interest in the Fourier-transformed data ($0.5 < R < 4$ Å) and therefore is irrelevant. It can be eliminated by Fourier filtering (smoothing) if desired. Comparison between partial sums of the data gives a more meaningful estimate of the noise within the pass band than does inspection of the unfiltered data.

Some useful information can be obtained by examination of Figure 1, however. The dominant, slowly varying structure

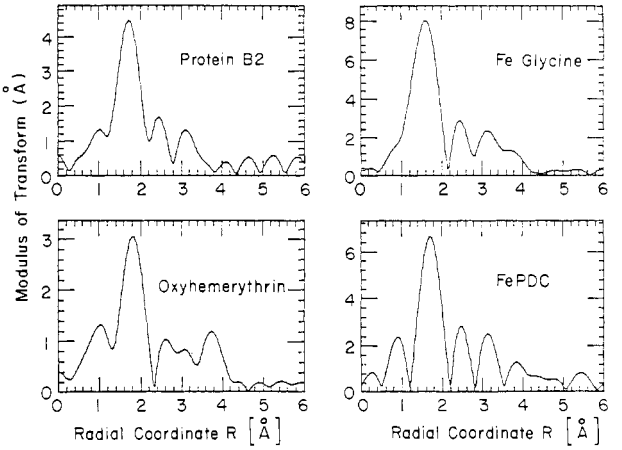

FIGURE 2: Fourier transforms of the EXAFS data of protein B2, oxyhemerythrin, Fe glycine, and Fe PDC. The transforms were performed over the k range 2.8–8.5 Å^{-1} with k^3 weighting.

is from the first coordination shell, and the higher shells give rise to smaller, more rapid oscillations. Substantial differences between the amplitudes of first and higher shell contributions of protein B2, oxyhemerythrin and the standards are evident. The larger first-shell amplitudes for the standards than for the proteins can be explained by a greater degree of radial order in the standards. A mean square variation in distance of 0.010 Å^2 would reduce the amplitude by a factor of 2 at k = 6 Å^{-1}. As described below, oxyhemerythrin also exhibits higher shell contributions resulting from histidine coordination.

It is apparent from Figure 1 that the first-shell phase of oxyhemerythrin leads that of protein B2, particularly at high k. The larger rate of increase of the phase for oxyhemerythrin indicates a larger average first-shell distance. The phase of protein B2 resembles more closely that of the Fe glycine and Fe PDC standards, which contain mainly oxygen in the first coordination shell and have average first-shell distances of 2.02 and 2.03 Å, respectively. The average distance in protein B2 is, however, substantially greater than in the Fe TIM standard (1.94 Å). Furthermore, the EXAFS amplitudes of Fe PDC and protein B2 clearly exhibit minima around k = 6 Å^{-1} (cf. also Figure 3), which indicates a beat from interference between rather different bond lengths within the first coordination shell. The dip occurs where $2k\Delta R\Delta = \pi$ (Martens et al., 1977), so the first shell in protein B2 consists of two subshells split by about 0.26 Å. The modest depth of the dip implies that most of the atoms are in one subshell, and only about one in the other. From X-ray diffraction it is known that in the Fe PDC standard five oxygen/nitrogen atoms are at an average distance of 2.08 Å and one oxygen is at 1.77 Å. The true difference in distance of 0.31 Å is in rough agreement with the analysis above. A similar situation occurs for oxyhemerythrin, but the first-shell beat is not so striking because of the larger relative contribution from higher shells.

These observations are confirmed by the Fourier transforms shown in Figure 2. The noise level corresponds roughly to the average transform magnitude for $R > 4$ Å in these materials. The first-shell peaks are shifted about −0.4 Å compared to the true iron–first-shell distance because of the k dependence of the back-scattering and central atom phase shifts. The transform peak position simply reflects the average slope of the phase shift in k space. The shift of −0.4 Å can be altered by beating and interference, however, because the phase slope varies strongly with k in that case. The first-shell peaks of the proteins and Fe PDC exhibit a low-R side lobe, while Fe glycine and Fe TIM do not. The low-R side lobe/peak did not vary significantly under change of the background sub-

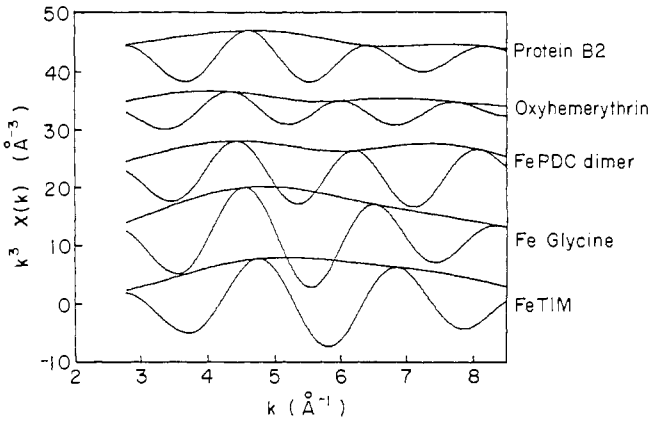

FIGURE 3: Fourier-filtered first-shell EXAFS data of protein B2, oxyhemerythrin, and standards. The inverse transforms were performed over the R range 0.4–2.2 Å except for oxyhemerythrin for which the range was shifted by 0.1 Å to 0.5–2.3 Å. The amplitude functions are overplotted. Spectra are displaced vertically for clarity.

traction parameters. It would seem reasonable to assign this peak to a short bond, but the bond length is too short to be compatible with an Fe–O distance in a μ-oxo bridge. It should, however, be noted that the peak could be shifted to lower R values because of interference with the main part of the first shell. In their EXAFS analysis of azidomethemerythrin, Hendrickson et al. (1982) excluded this peak from their R-space transform window, yet their fits still indicated the existence of a short bond. On the other hand, Elam et al. (1982) included this peak in their analysis of three different oxidized hemerythrins with similar results as those of Hendrickson et al. The peak may arise from contributions of $\mu_0(E)$ to the EXAFS (Holland et al., 1978), which are not divided out in the analysis because they are unknown in general. These effects generally oscillate slowly with energy (or not at all) and usually can be removed unambiguously, except when a short bond is present, as in the present analysis. However, even with perfect background subtraction these effects can introduce an amplitude modulation of the experimental EXAFS, which also may introduce side lobes. We have performed theoretical single-scattering calculations of the XANES of the central Fe atom alone as well as for a cluster containing six first-shell oxygens at a single distance. When these data were analyzed in the same manner as the experimental data, a low-R peak similar to that in the experimental data was found in the Fourier transform, even for the isolated-atom spectrum. This suggests that at least part of the low-R peak may arise from the energy dependence of $\mu_0(E)$. The strength of the peak in the Fourier transform depended on the nearest-neighbor bond length, because of the amplitude modulation imposed on the EXAFS by $\mu_0(E)$. The peak may be affected by a combination of other factors as well, including nonlinear contributions to the phase from breakdown of the plane wave approximation. Because of the ambiguities, it seemed most prudent to include the low-R side lobe with the main first-shell peak when back-transforming from R space into k space. All of the data were treated in this way. The Fourier-filtered data are shown in Figure 3.

The first-shell beats are more obvious after Fourier filtering (Figure 3). In addition to the dip in the amplitude, a sudden increase (rather than a decrease) in phase (data not shown) occurred at the beat. It is shown in the Appendix that this implies that, of the two subshells causing the beat, the subshell containing fewer atoms (one or two) is at the shorter distance. Alternatively, the positive curvature of the phase difference between protein B2 and the Fe glycine standard in the k range below the beat implies that the third cumulant is negative; i.e., the distribution of atoms in the first shell is skewed to shorter distances (Bunker, 1983). This also indicates the presence of a short bond distance within the first shell.

The Fourier-transformed data in Figure 2 indicate similarities and also significant differences between protein B2 and oxyhemerythrin. For example, the first-shell peak for oxyhemerythrin occurs at about 0.1 Å longer distance than for protein B2, which is a significant difference, and the peak is only about two-thirds as high. The higher transform peak intensity for protein B2 is most likely due to a smaller mean square disorder in the first coordination shell of its iron since a higher coordination number than in oxyhemerythrin (i.e., 6) is unlikely. An increase in the mean square disorder of approximately 0.006 Å^2 would give an amplitude reduction of about two-thirds for this range in k-space. About half of this difference of 0.006 Å^2 is expected since oxyhemerythrin was measured at room temperature and protein B2 at about 200 K. The remainder of the difference in Debye–Waller factor must be due to a slightly greater spread in first-shell distances in oxyhemerythrin than in protein B2. The sharp minimum at about 2.3 Å in the oxyhemerythrin spectrum indicates the presence of interference between the first-shell peak and the peak at about 2.6 Å. The greater degree of interference at 2.3 Å in the oxyhemerythrin spectrum than in the protein B2 spectrum is probably a consequence of the larger average first-shell distance in oxyhemerythrin. The first-, second-, and third-shell transform peak positions for protein B2 are very similar to those for the Fe PDC standard. The relative peak heights can be explained by a combination of a lower measurement temperature (80 K) together with a slightly lower static disorder for the Fe PDC compound than for protein B2.

Differences in the higher shell peak positions and heights are evident. The peaks at about 2.6 and 3.1 Å in the Fourier-transformed data of oxyhemerythrin are respectively assigned to a low-Z shell and a shell that includes the second iron atom (and admixed low-Z atoms) (Elam et al., 1982; Hendrickson et al., 1982). In the oxyhemerythrin spectrum, the contributions from these shells are not well resolved over the k-space transform range usable for protein B2. Similarly the peaks at about 2.5 Å can be reasonably assigned to four carbons at approximately 2.9 Å for both Fe glycine and Fe PDC. The peaks around 3.1 Å in the transformed spectra of both of these standards are primarily attributable to scattering from neighboring iron. The heights of these peaks are about twice as large as the corresponding peak for protein B2, which is itself about 50% larger than the peak in oxyhemerythrin. These values make sense. Each iron in the Fe glycine standard has two equidistant iron neighbors, which contribute to its peak, and the Fe–O–Fe angle is 120°. The forward scattering amplitude enhancement (focusing effect) is known to be insignificant at such an angle (Co et al., 1983), and the usual EXAFS formalism (eq 1) applies. In the Fe PDC standard, on the other hand, two iron atoms are linked by a linear (180°) μ-oxo bridge, so that the full effect of forward scattering enhancement is seen [cf. Co et al. (1983)]. This enhancement of the single iron atom's amplitude for Fe PDC gives about the same size transform peak as scattering from the two irons in Fe glycine. The ratio of the forward scattering amplitude to the back-scattering amplitude is largest at high values of k. When the k range is restricted (as it is in this work), the average enhancement is expected to be less than that observed over a wider range in k. Indeed, Co et al. (1983) observed a factor of 4.0 for the average amplitude enhancement in the

k range 4–16 Å^{-1}. It is also possible that part of the amplitude enhancement observed by Co et al. may have resulted from reduced disorder in the compounds of large bridging angle. For a given thermal variation in bridging angle, simple geometrical considerations show that the disorder σ^2 is proportional to $\cos^2(\theta/2)$, so that larger bridging angles result in less disorder. Since Co et al. did not allow the Debye–Waller factor to vary in their fits, such reduced disorder may have made a substantial contribution to their fourfold amplitude enhancement. For protein B2 the observed peak height is compatible with the presence of a single Fe neighbor that is not linearly bridged. The somewhat smaller peak height for oxyhemerythrin than for protein B2 probably occurs because of the higher measurement temperature in the former case.

The focusing effect also causes an apparent shift in distance that depends on the bridging angle. The true Fe–Fe distance in Fe PDC (3.54 Å) is 0.24 Å greater than in Fe glycine (3.30 Å), but the Fe peaks in the Fourier transforms occur at nearly the same position. Co et al. have reported an apparent distance shift (i.e., difference between apparent distance from the EXAFS analysis and true distance) of −0.22 Å for Fe–O–Fe compounds with 180° bridging angle and negligible shift for compounds with an angle around 120°. This is consistent with the observed transform peak positions for Fe glycine and Fe PDC.

Oxyhemerythrin also exhibits a prominent transform peak at about 3.8 Å, which has been assigned to scattering from the distal nitrogen and carbon of histidine imidazole rings. The large size of the peak was explained as a consequence of reduced thermal motion from the rigid ring and the focusing effect (Bunker et al., 1982). This histidine peak is conspicuously absent for the present protein B2 spectra, or at least buried in the noise. This may be so because of a reduced number of histidine ligands, or alternatively a quenching of their signal by a tilted conformation, which would reduce the forward scattering enhancement. If histidines are present and not tilted, the noise level provides an upper bound of the number of histidines of about 1.5/Fe. There is no evidence for the presence of histidine ligands from these data, but the possibility of a total of about three for the two Fe sites cannot be ruled out. Spectra of improved signal-to-noise ratio should answer this question.

Quantitative Analysis. The positions and widths of the higher shell transform peaks (Figure 2) permitted the use of the same R-space filtering windows for protein B2 and the standards. Some interference between the higher shells (especially for Fe PDC) is evident from the sharpness of the valleys, but errors from this effect are expected to cancel out reasonably well because the data being compared are so similar and the windows are the same. For oxyhemerythrin the first-shell window width was kept the same as for the other materials, but the center was shifted to account for the difference in peak position. No attempt to isolate the higher shells for oxyhemerythrin was made for this narrow k-space transform range. The R-space windows used for protein B2 and the standards were 0.4–2.2, 2.2–2.8, and 2.8–3.5 Å for the first, second, and third shells, respectively. The narrow widths used for the higher shell windows greatly reduced the information content, and unique parameters were not obtainable for those shells. R-Space windows were flat-topped with ±0.1 Å cosine-squared tapers on each side. The filtered first-shell data are shown in Figure 3.

First Shell. The amplitudes and phases of the model compounds obtained by Fourier filtering were used to fit the filtered protein B2 data according to the standard EXAFS

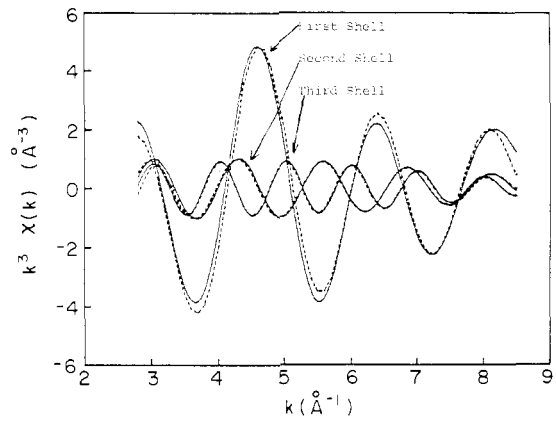

FIGURE 4: Typical fits to the Fourier-filtered EXAFS data of protein B2 using the nonlinear fitting method. The least rapidly oscillating curve is for the first shell, and the most rapidly oscillating curve is for the third shell. The solid lines are the filtered protein B2 data, and the dashed lines are the fits.

equation, eq 1 (Stern et al., 1975). The use of first-shell amplitudes and phases to fit to higher shells introduces systematic errors because of the breakdown of the plane wave approximation implicit in eq 1, and therefore this practice was not followed. No more than four parameters were floated at a time in any fit. The number of degrees of freedom $2\Delta k\Delta R/\pi$ in the first-shell-filtered data was about 7 (of which 4 were used). Different starting points were chosen in the fitting process to search for local minima of the residual sum of squares. Several such minima were found. Most of them corresponded, however, to unacceptably poor phase fits, even if they gave rise to a beat as required for a good amplitude fit. Beats occur when $2k\Delta R = (2M + 1)\pi$ with M integer, and this class of solutions (e.g., five atoms at 2.11 Å, one at 1.21 Å) corresponded to $M = 1$ rather than to the physical solution with $M = 0$. An independent analysis of the first-shell data using a wider k-space range and a weighting function $[k^5 \exp(-0.04k^2)]$ causing effective damping at high k values to suppress the noise yielded results identical with those presented here.

In the following discussion a special notation will be used to describe the fits. For example, a two-shell fit with the coordination numbers fixed to 5 and 1, respectively, while floating the average distances R and the variances in distances SS (σ^2) will be written ⟨N1 = 5, N2 = 1; R1, R2, SS1, SS2⟩. Constrained parameters are written before the semicolon, and floating parameters are written after it. A single distance fit in which N, R, and SS are floated will be written ⟨N, R, SS⟩.

Several test fits were done to check consistency. A single-shell fit ⟨N, R, SS⟩ of the Fe PDC first-shell data was made of the Fe glycine compound as standard. This gave an unacceptable fit, as expected because the large (0.3-Å) difference in distance between the bridging oxygen (at 1.77 Å) and the other first-shell atoms in Fe PDC (at an average of 2.08 Å) results in an obvious beat within the data range (cf. Figure 4), and this beat cannot be reproduced in a single-shell fit. The two-shell model ⟨N1 = 1, N2 = 5; R1, SS1, R2, SS2⟩ gave a good fit, with distances of R1 = 1.78 ± 0.03 Å and R2 = 2.08 ± 0.03 Å. The error estimates refer to fitting errors only. The distances reported on the basis of X-ray crystallographic analysis (Ou et al., 1978) are 1.77 and 2.08 Å. Another test fit using the two-distance model was made to the first-shell data of oxyhemerythrin. The longer distance subshell was supposed to contain three oxygen and two nitrogen atoms at the same distance and with the same σ^2. This fit gave the result R1 = 2.12 ± 0.03 Å, SS1 = 0.0065 ± 0.0022 Å^2, R2

Table I: Parameters Estimated for the Iron Center in Protein B2 from EXAFS Analysis[a]

first-shell fits					
N1	R1 (Å)	SS (Å^2)	N2	R2 (Å)	SS (Å^2)
5	2.04 ± 0.07	0.005 ± 0.005	1	1.78 ± 0.07	−0.002 ± 0.005
4	2.04 ± 0.07	0.002 ± 0.003	1	1.78 ± 0.07	−0.002 ± 0.005
4	2.05 ± 0.07	0.002 ± 0.003	2	1.80 ± 0.07	+0.006 ± 0.008

second shell (nonunique solution): N = 3–4; R = 2.93 Å; SS = 0.009 Å^2

third shell (nonunique solution): N = 1 Fe; R = 3.26–3.48 Å; SS = 0.006 Å^2

[a] The values shown are composites of values obtained from many fits, each of which was judged to give an acceptable fit within the noise and systematic errors. Differences between sums-of-squares values for the acceptable fits shown are not sufficiently significant to favor one acceptable solution over another. Meaningful error limits could not be obtained for the second and third shell because the number of degrees of freedom in the filtered data was equal to the number of parameters in the fit. SS (σ^2) values are relative to the Fe glycine standard. The known structural disorder in the standards has been compensated for, but the unknown thermal disorder has not. Negative SS values indicate less thermal disorder in protein B2 than in the Fe glycine standard.

= 1.83 ± 0.03 Å, and SS2 = −0.0041 ± 0.0033 Å^2. The error estimates refer to fitting errors only. These values are consistent with the previously reported results R1 = 2.16 ± 0.05 Å, SS1 = 0.005 ± 0.001 Å^2, R2 = 1.83 ± 0.05 Å, and SS2 = −0.003 ± 0.005 Å^2 (Elam et al., 1982).

As was found for the μ-oxo-bridged Fe PDC compound, attempts to fit the single-shell model ⟨N, R, SS⟩ to the first-shell data for protein B2 with Fe glycine as standard gave unsatisfactory results, but the two-distance model ⟨N1 = 1, N2 = 5; R1, SS1, R2, SS2⟩ was successful. A number of fits with varying coordination numbers totaling six and five atoms were performed with various initial guesses for parameters. A summary of the results is given in Table I. Typical acceptable fits to the first-, second-, and third-shell-filtered data are shown in Figure 4. The differences between the fits and the data are attributed to noise and systematic errors from background subtraction and Fourier filtering. In Figure 5 typical first-, second-, and third-shell fits are summed together and compared with the multishell protein B2 data, which for clarity were smoothed to eliminate the high-frequency noise. This test confirms that no inconsistencies in the data analysis arise as a consequence of Fourier filtering and fitting to each shell separately.

From Table I, it is obvious that several models assuming 5- or 6-coordinated iron are consistent with the present data. Fourfold coordination can be ruled out, however. Since two inequivalent Fe sites are present (Atkin et al., 1973), it is possible that one iron has five ligands and the other, six. We performed a series of fits in which the partitioning of six or five atoms between the subshells was systematically varied: ⟨N1 = 1–5, N2 = 6 − N1; R1, SS1, R2, SS2⟩ and ⟨N1 = 1–4, N2 = 5 − N1; R1, SS1, R2, SS2⟩. Acceptable fits were obtained with partitions of four/one, five/one, and four/two atoms in the longer/shorter distance subshell. When more than two atoms were placed in the short-distance subshell, the fitting procedure tried to compensate by strongly increasing the Debye–Waller factor SS value for the short bond (reducing the amplitude) and driving the SS value for the long bond strongly negative (thereby increasing the amplitude). This occurred because the N and SS parameters were highly correlated. The best values of SS for some of these unacceptably poor fits were so large as to invalidate the two-distance

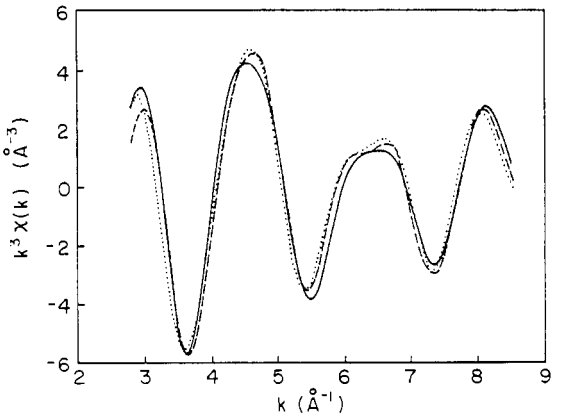

FIGURE 5: Comparison of Fourier-smoothed EXAFS data of protein B2 as shown in Figure 1 (solid curve) with multishell fits assuming different proportions of nitrogen and oxygen atoms in the first coordination shell. The inverse transform range in filtering (0.4–3.8 Å) included all shells but excluded high-frequency noise. The dotted and dashed curves were synthesized by means of the standards Fe glycine and Fe TIM, which contain oxygen and nitrogen in their first coordination shell, respectively. The dotted curve was obtained by assuming a first coordination shell with one oxygen atom at 1.76 Å (SS = −0.001 Å^2) and five oxygen atoms at 2.05 Å (SS = 0.006 Å^2). For the dashed curve on the other hand this shell was assumed to contain a mixture of three oxygen and two nitrogen atoms at an average distance of 2.04 Å (SS = 0.003 Å^2) and one oxygen atom at 1.77 Å (SS = −0.003 Å^2). The second- and third-shell parameters were the same for both curves and corresponded to four carbon atoms at 2.98 Å (SS = 0.009 Å^2) and 1.35 iron atoms at 3.29 Å (SS = 0.006 Å^2), respectively.

(Gaussian Debye–Waller factor) model (Bunker, 1983). Additional fits with mixtures of nitrogens and oxygens were performed, but it was not possible to distinguish nitrogen from oxygen ligation for the present protein B2 data set. The variations in parameters (primarily SS) that resulted from the uncertainty in ligand type were folded into the errors quoted.

Second Shell. The occurrence of the second-shell peaks at about 2.5 Å in the Fourier transforms for protein B2 and the models suggested that they may be of similar origins. For the Fe PDC complex the peak is due to four carbons in a narrow coordination shell at 2.96-Å distance from the iron. In Fe glycine each iron is surrounded by four carbons at 2.99 Å, two irons at 3.30 Å, and four oxygens at 3.40 Å. Single-shell fits ⟨N, R, SS⟩ were performed to the second-shell data for protein B2 using Fe PDC as the standard. The number of degrees of freedom of the filtered data was about 3 due to the k- and R-space windows used for the transforms. Acceptable fits were obtained for three or four carbons, with SS = 0.006 ± 0.004 Å^2, at an average distance of 2.91 ± 0.07 Å. Although this is an acceptable and reasonable solution, it is by no means unique. Because of the narrow filtering windows and the resulting high degree of smoothing the best fit was misleadingly good. An infinitely narrow R-space window would yield a pure sine wave and zero error limits, but all physical meaning would be lost. The error bars for the average distance that were estimated from the curvature and the minimum value of the sum of squares function were ±0.02 Å. In this case more realistic error limits (±0.07 Å) were obtained by the partial sum method and estimating the limits from the variation in distance between acceptable fits.

Third Shell. As discussed above, the Fourier transform peaks at about 3.1 Å in oxyhemerythrin, Fe glycine, and Fe PDC are assigned to Fe–Fe scattering, possibly with some admixed contribution from low-Z atoms. The bridging (Fe–O–Fe) angle in Fe glycine is 120°, the forward scattering/focusing effect was accordingly considered to be negligible.

On the other hand, the Fe PDC compound exhibits a maximal focusing effect because its bridging angle is 180° (scattering angle zero). The phases of Fe PDC and Fe glycine were directly compared by the ratio method and also by nonlinear fitting with the hypothetical model ⟨N, R, SS⟩. The apparent distance shift for Fe PDC (i.e., the difference between the apparent and the true distance) obtained from fitting was −0.22 ± 0.05 Å; a value of −0.23 ± 0.05 Å was determined from the slope of the phase difference. The focusing effect also appeared to introduce a constant negative phase shift of about 1 rad, as well as some positive curvature to the phase difference between Fe PDC and Fe glycine. Because of this, the phase fit was not good for a single-shell fit the third-shell Fe PDC data when Fe glycine was used as a reference. The amplitude fit was good, however, and indicated an amplitude enhancement of 1.75 ± 0.75 for Fe PDC. This error limit is large because of the correlations between N and SS. The ratio method tends to decouple such correlations, and the value obtained by that method was 1.85 ± 0.2 after compensation for the differences in number of irons and the distance. For the purpose of comparison with the results of to Co et al. the fit ⟨SS = 0; N, R⟩ was also performed. The amplitude fit was poor, and the best fit amplitude enhancement was 1.79 ± 0.45. The smaller error bar compared to the fit ⟨N, R, SS⟩ simply reflects the suppression of correlations by elimination of a parameter and does not take into account systematic errors from use of the oversimplified model ⟨N, R⟩. As mentioned above, the amplitude enhancement differs from the values obtained by Co et al. who report a fourfold, rather than a twofold amplitude enhancement for compounds with an Fe–O–Fe angle of 180°. No amplitude enhancement is observed for 120° bridged compounds. Since the focusing enhancement is larger at high energies, it seems likely that the larger amplitude enhancement found by Co et al. stems in part from their wider k range.

Fits of the form ⟨N, R, SS⟩ to the third-shell data of protein B2 were done with Fe glycine and Fe PDC as standard compounds. Good fits were obtained with Fe glycine as the standard, but using Fe PDC resulted in a poor fit (a factor of 10 worse in residual sum of squares), with a residual phase curvature similar to that observed in comparison of the two standards. This strongly suggests that the bridging angle in protein B2 is much closer to 120° (as in Fe glycine) than 180° (as in Fe PDC). The estimated Fe–Fe distance in protein B2 obtained by using Fe glycine as the standard was 3.26 Å, with a fitting error of only ±0.01 Å but an estimated total error of ±0.07 Å. The distance obtained by the ratio method was 3.26 ± 0.07 Å. This value of 3.26 Å represents a lower bound on the true distance because of the bridging angle dependent apparent distance shift described above. The apparent number of iron atoms in the shell obtained from nonlinear fitting was 1.24 ± 0.40, while 1.35 ± 0.15 was obtained from the ratio method. Since there is only one neighboring iron, the average enhancement factor is about 1.3.

Discussion

First Shell. Our analysis of the EXAFS data for the first coordination shell in protein B2 indicates that each iron atom of its dimeric iron center is coordinated to either five or six oxygen or nitrogen ligands. There is no evidence for sulfur coordination.

A successful interpretation of the EXAFS data requires at least one iron ligand in a subshell at a short distance around 1.75–1.80 Å. Similar distances have been reported for the Fe–O bond of the μ-oxo bridge in oxyhemerythrin (Elam et al., 1982) and in two methemerythrin derivatives (Elam et al., 1982; Hendrickson et al., 1982; Stenkamp et al., 1984). For a number of μ-oxo-bridged dimeric iron model complexes the Fe–O bond length falls in the range 1.76–1.82 Å (Ou et al., 1978; Thich et al., 1982). This is also true for model complexes, which in addition to the μ-oxo bridge contain two bridging carboxylate groups (Wieghardt et al., 1983; Armstrong et al., 1984). Accordingly we assign the short distance in protein B2 to the Fe–O bond of a μ-oxo bridge. Evidence supporting such a structure has previously been derived from light absorption (Atkin et al., 1973; Petersson et al., 1980), Mössbauer (Atkin et al., 1973), magnetic susceptibility (Petersson et al., 1980), and resonance Raman (Sjöberg et al., 1982) studies.

The remaining atoms in the first coordination shell are at a longer average distance, 2.04 Å. It is not possible to distinguish between oxygen and nitrogen atoms in this subshell from the present EXAFS data. An upper limit of three histidine nitrogens for the two iron atoms together can however be estimated from the intensity of the EXAFS peak at 3.8 Å in the Fourier transform, as described in the quantitative analysis. The alternative explanation for the low peak intensity, i.e., a tilted histidine conformation resulting in unfavorable conditions for forward scattering, has to our knowledge not been observed, and we find this possibility less likely. The limit above finds support in a comparison of amino acid sequences for the small subunit of reductases from four different species (Sjöberg et al., 1985). If it is assumed that functionally important amino acids, e.g., iron ligands, are conserved, each polypeptide can contribute a maximum of two histidine ligands. The potential candidates are His-118 and His-241 in each chain.

The longer distance subshell in oxyhemerythrin and some methemerythrins is found at a distance of 2.15–2.16 Å (Elam et al., 1982). We consider the distance difference of about 0.1 Å between protein B2 and the oxidized forms of hemerythrin to be significant. As pointed out in the qualitative analysis, the first coordination shell in oxyhemerythrin is also slightly more disordered than that in protein B2. Those differences may reflect different structural restraints imposed by the protein, but they may also to some extent reflect that a larger number of oxygens are coordinated to the iron center in protein B2 than in the hemerythrin derivatives. Recently the structures have been characterized for some tribridged dimeric iron complexes, which accurately model the active site of oxidized hemerythrins. In these compounds the Fe–O bond lengths for bridging carboxylates were found to fall in the range 2.03–2.05 Å (Wieghardt et al., 1983; Armstrong et al., 1984). Slightly longer distances were reported for Fe–N bonds. Thus, trans to bridging carboxylate, Fe–N bonds were found to be in the range 2.14–2.16 Å and trans to the μ-oxo bridge in the range 2.18–2.21 Å. In the monobridged Fe PDC compound the Fe–O distance of a nonbridging carboxylate was reported to be 2.09 Å (Ou et al., 1978). Water coordination generally results in Fe–O bond lengths in the range 2.05–2.13 Å (Thundathil et al., 1977; Ou et al., 1978), and the Fe–O distance is probably shorter when a hydroxide is bound. Apparently, in model complexes, which are closely related to the iron centers of protein B2 and the oxidized hemerythrins, the Fe–O bonds seem to be slightly shorter than the Fe–N bonds and this relationship might to some extent be preserved in the proteins. However, X-ray crystallographic studies on metazidohemerythrin are consistent with distances in approximately the same range for Fe–N as well as Fe–O bonds (Stenkamp et al., 1984). This indicates that a possible systematic difference in bond lengths is overshadowed by the

influence from the protein backbone. The strain imposed on the active site in protein B2 could be less, as a consequence of its location at the interface between the two polypeptide chains. Another possibility is, however, that the X-ray crystallographic results for metazidohemerythrin are due to the uncertainty inherent in structure determinations on large protein molecules.

From the observed sequence homologies (Sjöberg et al., 1985), it is suggested that Glu-115 and Asp-237 or Glu-238 of each polypeptide chain could contribute oxygen ligands to the iron center. Furthermore, there should be a hydroxide ligand, since a recent resonance Raman study (Sjöberg et al., manuscript in preparation), shows that both native and hydroxyurea-treated protein B2 exhibit an Fe–OH vibration at 598 cm^{-1}, which is shifted 22 cm^{-1} to lower energy on ^{18}O substitution. It was not possible to tell from the resonance Raman data whether there is more than one hydroxide ligand present.

In the case of six ligands in the first coordination shell, our data could also be compatible with two short bonds of rather different length, i.e., 1.72 and 1.88 Å. The longer distance could be associated with the Fe–O bond for the hydroxide ligand. However, 1.72 Å would be a very short Fe–O distance for the bridging oxygen, and we find this possibility less likely.

Second Shell. The EXAFS peak around 2.5 Å in the Fourier transform probably originates from about four low-Z (presumably carbon) atoms at about 2.9 Å. Possible candidates are the C2 and C4 atoms of histidine as well as the carboxylate carbons of glutamate and aspartate.

Third Shell. Our EXAFS analysis shows an apparent distance separation of 3.26 Å between the μ-oxo-bridged iron atoms in protein B2. With the assumption that the two Fe–O bond lengths are equal, simple geometrical considerations give a bridging angle (Fe–O–Fe) of 130° for a Fe–O distance of 1.80 Å. This apparent Fe–Fe distance is however not necessarily equal to the true distance. It could also be a consequence of a somewhat longer separation combined with a distance reduction due to forward scattering. In their systematic investigation of a number of μ-oxo-bridged dimeric iron complexes, Co et al. (1983) found that Fe–Fe distances evaluated from EXAFS analysis and X-ray crystallographic results agrred for bridging angles below 120°. Progessively shorter distances were determined from the EXAFS analysis as the bridging angle was increased above this value, with a maximum distance reduction of 0.22 Å at an angle of 180°. In agreement we find a distance reduction around 0.22–0.23 Å for the linear Fe PDC compound, when Fe glycine with a bridging angle of 120° is used to model its iron shell. As a crude estimate, the upper limits of the true Fe–Fe distance in protein B2 would thus be 3.48 Å, corresponding to a bridging angle of 150°.

Co et al. (1983) also reported an angular-dependent enhancement of the Fe EXAFS amplitude for bridging angles above 120° due to forward scattering. A maximum enhancement factor of 4.0 was found for an Fe–O–Fe angle of 180°, while in the present analysis a factor of 1.8 is estimated for the linear Fe PDC compound. The discrepancy is probably related to the different k ranges in the data acquisition. The factor around 1.3 obtained for protein B2 indicates a bridging angle significantly below 180°.

In modeling the iron shell of protein B2 we found better fits using Fe glycine as the standard, than with the Fe PDC compound. The EXAFS phase of the linear Fe PDC compound exhibited a strong negative-phase curvature relative to the Fe glycine compound, which has a bridging angle of 120°. The protein B2 data showed no such phase curvature.

In summary, our results for the third coordination shell in protein B2 are compatible with an Fe–Fe distance in the range 3.26–3.48 Å and a bridging angle between 130 and 150°. The close similarity to the Fe glycine compound indicates that the true values are probably found at the lower limits of those ranges.

Interestingly, the Fe–O–Fe angle has also been estimated in a recent resonance Raman study. Following the analysis by Wing and Callahan (1969) and assuming as singly bridged iron center, a bridging angle of 138° was estimated from the magnitude of the shifts to lower energy in $H_2{}^{18}O$ for the Fe–O–Fe symmetric and asymmetric stretches (Sjöberg et al., 1986). Since methemerythrins show analogous shifts of their corresponding Fe–O–Fe vibrations on exchange to $H_2{}^{18}O$ (Freier et al., 1980; Shiemke et al., 1984), it was suggested that a triply bridged iron center as in oxidized hemerythrins was also present in protein B2 (Sjöberg et al., 1986).

The Fe–Fe distance in protein B2 appears to be slightly longer than that in the oxidized forms of hemerythrin. In met- and metazidohemerythrin distances of 3.21 and 3.25 Å have been determined from X-ray crystallography at 2.0-Å resolution (Stenkamp et al., 1983, 1984). EXAFS analysis originally resulted in Fe–Fe distances of 3.49 Å (Elam et al., 1982) and 3.38 Å (Hendrickson et al., 1982) for metazidohemerythrin. The slight disagreement between the two methods was resolved by incorporating carbon back-scatterers in the EXAFS fitting for the iron shell, whereby the distances 3.20 and 3.24 Å (Co, 1983; J. Loehr, personal communication) were obtained. A similar effect may be operative in the present protein B2 data, but this can only be investigated further with data of improved signal-to-noise ratio. The Fe–Fe distances found in the triply bridged model compounds, 3.14 Å (Armstrong et al., 1984) and 3.06 Å (Wieghardt et al., 1983), are shorter than those found in the proteins. It should be noted that the bridging angles in these compounds, as well as in the methemerythrins, fall in the range 123–135° (Wieghardt et al., 1983; Armstrong et al., 1984; Stenkamp et al., 1984) whereas in the number of model compounds with a single μ-oxo bridge it is larger than 139° (Thich et al., 1982). The range found for the bridging angle in protein B2 would thus be compatible with both structures.

Added in Proof: We have recently become aware of a letter (Scarrow et al., 1986) describing a study very similar to ours (Bunker et al., 1986) with consistent results. The analysis described in the present paper is more complete, however. Scarrow et al. did not derive error estimates from their data, nor did they consider systematic errors from multiple scattering effects. These omissions make it difficult to determine the significance of their parameter estimates. Nevertheless, the close similarity of the results obtained by independent groups using different methods strongly reinforces the conclusions.

ACKNOWLEDGMENTS

We are very grateful to P. Reichard for taking the right steps in the beginning of this study to initiate and encourage the collaboration. We are also very grateful to W. T. Elam for freely providing his oxyhemerythrin and model compound EXAFS data.

APPENDIX

The total EXAFS phase ϕ for a coordination shell comprising two subshells of amplitudes A_1, A_2 and phases ϕ_1, ϕ_2 can be written (Bunker, 1983)

$$\phi = \bar{\phi} + \tan^{-1} Z$$

where

$$\bar{\phi} = \frac{\phi_1 + \phi_2}{2}$$

$$Z = \left[\left(\frac{A_1 - A_2}{A_1 + A_2}\right)\tan\left(\frac{\Delta\phi}{2}\right)\right]$$

$$\Delta\phi = \phi_1 - \phi_2$$

At a beat, i.e., where $\Delta\phi \cong (2n + 1)\pi$ with n integer, the phase ϕ rapidly increases or decreases. Neglecting the variation in A_1 and A_2, we obtain

$$\frac{d\phi}{dk} \cong \frac{d\bar{\phi}}{dk} + \left[\frac{1 + \tan^2(\Delta\phi/2)}{1 + Z^2}\right]\left(\frac{A_1 - A_2}{A_1 + A_2}\right)\frac{d\Delta\phi}{dk}$$

The term in square brackets is never negative. Since

$$\frac{d\Delta\phi}{dk} \cong 2(R_1 - R_2) \qquad A_1 - A_2 \cong \frac{N_1}{R_1^2} - \frac{N_2}{R_2^2}$$

where N and R are the coordination number and distance, it is evident that the change in phase at the beat has the same sign as the quantity

$$\left(\frac{N_1}{R_1^2} - \frac{N_2}{R_2^2}\right)(R_1 - R_2)$$

Thus, if the smaller amplitude subshell occurs at the shorter distance, the phase change is positive.

Registry No. Fe glycine, 54816-00-1; Fe PDC, 67477-28-5; Fe TIM, 43223-41-2; Fe, 7439-89-6; ribonucleotide reductase, 9047-64-7.

REFERENCES

Armstrong, W. H., Spool, A., Papaefthymiou, G. C., Frankel, R. B., & Lippard, S. J. (1984) *J. Am. Chem. Soc. 106*, 3653–3667.

Atkin, C. L., Thelander, L., Reichard, P., & Lang, G. (1973) *J. Biol. Chem. 248*, 7464–7472.

Bunker, B. A., & Sayers, D. E. (1986) in *Extended X-ray Absorption Fine Structure* (Prins, R., & Koningsberger, D., Eds.) Wiley, New York (in press).

Bunker, G. B. (1983) *Nucl. Instrum. Methods Phys. Res. 207*, 437–444.

Bunker, G. B., Stern, E. A., Blankenship, R., & Parson, W. W. (1982) *Biophys. J. 37*, 539–551.

Bunker, G. B., Sjöberg, B.-M., Reichard, P., Petersson, L., Chance, B., & Chance, M. (1986) *Fed. Proc., Fed. Am. Soc. Exp. Biol. 45*, 1601.

Co, M. S. (1983) Ph.D. Dissertation, Stanford University.

Co, M. S., Hendrickson, W. A., Hodgson, K. O., & Doniach, S. (1983) *J. Am. Chem. Soc. 105*, 1144–1150.

Ehrenberg, A., & Reichard, P. (1972) *J. Biol. Chem. 247*, 3485–3488.

Elam, W. T., Stern, E. A., McCallum, J. D., & Sanders-Loehr, J. (1982) *J. Am. Chem. Soc. 104*, 6369–6373.

Freier, S. M., Duff, L. L., Shriver, D. F., & Klotz, I. M. (1980) *Arch. Biochem. Biophys. 205*, 449–463.

Hendrickson, W. A., Co, M. S., Smith, J. L., Hodgson, K. O., & Klippenstein, G. L. (1982) *Proc. Natl. Acad. Sci. U.S.A. 79*, 6255–6259.

Holland, B. W., Pendry, J. B., Pettifer, R. F., & Bordas, J. (1978) *J. Phys. C 11*, 633–642.

Joelson, T., Uhlin, U., Eklund, H., Sjöberg, B.-M., Hahne, S., & Karlsson, M. (1984) *J. Biol. Chem. 259*, 9076–9077.

Lammers, M., & Follman, H. (1983) *Struct. Bonding (Berlin) 54*, 27–91.

Larsson, A., & Sjöberg, B.-M. (1986) *EMBO J. 5*, 2037–2040.

Lee, P. A., Citrin, P. H., Eisenberger, P., & Kincaid, B. M. (1981) *Rev. Mod. Phys. 53*, 789–806.

Martens, G., Rabe, P., Schwentner, N., & Werner, A. (1977) *Phys. Rev. Lett. 39*, 1411.

Ou, C. C., Wollmann, R. G., Hendrickson, D. N., Potenza, J. A., & Schugar, H. J. (1978) *J. Am. Chem. Soc. 100*, 4717–4724.

Petersson, L., Gräslund, A., Ehrenberg, A., Sjöberg, B.-M., & Reichard, P. (1980) *J. Biol. Chem. 255*, 6706–6712.

Scarrow, R. C., Maroney, M. J., Palmer, S. M., Que, L., Salowe, S. P., & Stubbe, J. (1986) *J. Am. Chem. Soc. 108*, 6832–6834.

Shiemke, A. K., Loehr, T. M., & Sanders-Loehr, J. (1984) *J. Am. Chem. Soc. 106*, 4951–4956.

Sjöberg, B.-M., & Gräslund, A. (1983) *Adv. Inorg. Biochem. 5*, 87–111.

Sjöberg, B.-M., Loehr, T. M., & Sanders-Loehr, J. (1982) *Biochemistry 21*, 96–102.

Sjöberg, B.-M., Eklund, H., Fuchs, J. A., Carlson, J., Standart, N. M., Ruderman, J. V., Bray, S. J., & Hunt, T. (1985) *FEBS Lett. 183*, 99–102.

Sjöberg, B.-M., Hahne, S., Karlsson, M., Jörnvall, H., Göransson, M., & Uhlin, B.-E. (1986) *J. Biol. Chem. 261*, 5658–5662.

Sjöberg, B.-M., Sanders-Loehr, J., & Loehr, T. (1987) *Biochemistry* (in press).

Stenkamp, R. E., Sieker, L. C., & Jensen, L. H. (1983) *Acta Crystallogr., Sect. B: Struct. Crystallogr. Cryst. Chem. B39*, 697–703.

Stenkamp, R. E., Sieker, L. C., & Jensen, L. H. (1984) *J. Am. Chem. Soc. 106*, 618–622.

Stern, E. A. (1974) *Phys. Res. B 10*, 3027–3037.

Stern, E. A., Sayers, D. E., & Lytle, F. (1975) *Phys. Rev. B 118* 4836–4846.

Thelander, L., & Reichard, P. (1979) *Annu. Rev. Biochem. 48*, 133–158.

Thich, J. A., Toby, B. H., Powers, D. A., Potenza, J. A., & Schugar, H. J. (1982) *Inorg. Chem. 20*, 3314–3317.

Thundathil, R. V., Holt, E. M., Holt, S. L., & Watson, K. J. (1977) *J. Am. Chem. Soc. 99*, 1818–1823.

Wieghardt, K., Pohl, K., & Gebert, W. (1983) *Angew. Chem., Int. Ed. Engl. 22*, 727.

Wing, R. M., & Callahan, K. P. (1969) *Inorg. Chem. 8*, 871–874.